Journal of Control, Automation and Electrical Systems
https://doi.org/10.1007/s40313-025-01165-6

A New Accurate and Robust Method Based on Deep Neural Networks for Fault Location in HVDC Systems

Victor Luiz Merlin[1] · Ricardo Caneloi dos Santos[1] · Ahda Pionkoski Grilo Pavani[1] · José Carlos Melo Vieira[2]

Received: 5 November 2024 / Revised: 30 January 2025 / Accepted: 17 March 2025

Abstract

This paper proposes a new method based on deep neural networks and direct-current voltage signal for fault location in high voltage direct current systems. An accurate performance of the fault location scheme has crucial role, enabling that planned actions can be taken to restore the power grid as soon as possible. In general, most of current methods employ communications links and/or require additional hardware processing current and voltage signals, as this is a complex function potentially affected by the control loops present in the converter substations. The proposed solution uses only voltage local measurements and a reasonable sampling frequency, which ensures its applicability. Performing an intelligent signal processing, the power system reliability and availability can be improved, without additional devices or communication links. The proposed method takes advantage of the high capability of neural networks for pattern recognition, associating the frequency spectrum of faulted signals to specific fault locations. The training process is detailed, and the definition of the most suited neural network architecture is presented. The method is validated by using different HVDC systems, different fault types and fault resistances. The results reveal the good performance and robustness of the proposed method and its potential for application for real scenarios.

Keywords HVDC systems · Fault location · Deep neural networks · Intelligent protection

1 Introduction

Nowadays, high voltage direct current (HVDC) systems are considered a consolidated technology for transmitting power through long distances. Despite several advantages over high voltage alternating current (HVAC) systems, new challenges are posed when considering HVDC systems. One of them is related to fault location function, which plays a vital role in protection schemes, collaborating to increase the electrical system availability (Anderson et al., 2021).

An accurate fault location scheme allows taking quick and proper actions to restore the HVDC system. However, factors such as long distances, operating conditions, control systems, among others, make the fault location a very complex task. Therefore, this issue draws the attention of many researchers that have been considering intelligent solutions to improve the existing fault location schemes, which are mostly based on traveling wave (TW) theory. In fact, solutions based on artificial intelligence are a promising way to address this kind of complex problems, overcoming some limitations of the conventional solutions (Jovcic et al., 2011).

Indeed, while TW-based methods require high sampling rates and are significantly affected by noise and high values of fault resistance, intelligent solutions can learn by data, are robust, efficient and accurate. These important characteristics are suitable for complex scenarios, as the ones imposed by the challenges related to HVDC systems (Li & He, 2020).

In Ye et al. (2021), it is presented a method based on wavelet transform (WT) and deep belief network (DBN) for fault location in DC transmission lines, where firstly the WT is used to decompose the original voltage fault signal, and then the low- and high-frequency components are used to train different DBNs models. Yang et al. (2017) propose the use of artificial neural network (ANN) for fault location in a three terminal HVDC system. In this case, specific high-frequency components are extracted by discrete Fourier

✉ Ricardo Caneloi dos Santos
ricardo.santos@ufabc.edu.br

[1] Federal University of ABC, Av. Dos Estados, 5001, Santo André, SP 09210-580, Brazil

[2] São Carlos School of Engineering, University of São Paulo, Av. Trabalhador São-Carlense, 400, São Carlos, SP 13566-590, Brazil

Published online: 08 April 2025

transform (DFT) and applied to a previously trained ANN responsible for locating the fault in the DC transmission line. A hybrid fault location scheme based on adaptive neuro-fuzzy inference system (ANFIS) is proposed in Rohani and Koochaki (2020), which uses fault current signals for estimating the fault distance in a DC transmission line of 250 km. Promising results were achieved in Lan et al. (2019) using convolutional neural networks (CNN) for fault location, considering unsynchronized two-end measurements. Hao et al. (2018) propose an intelligent scheme based on support vector regression for fault location in DC transmission lines, by using fault features captured with Hilbert–Huang transform (HHT) as input signals. An algorithm based on ANN for fault location in a low voltage DC microgrid is proposed by Yang et al. (2016), which uses current samples from the DC microgrid terminals as inputs to the previously trained ANN. On the same line, Abdali et al. (2019) propose and implement in hardware an intelligent algorithm based on ANN for fault location in a low voltage DC microgrid, by processing current signals from the microgrid terminals. In Ankar and Yadav (2020), a new approach for fault distance estimation in CSC-HVDC systems is presented, employing discrete wavelet transform (DWT) for feature extraction of faulted signals and Gaussian process regression (GPR) for fault estimation. A proposal based on ANN and similarity concept for fault location in CSC-HVDC systems is proposed in Silva et al. (2019), while Arita Torres et al. (2022) presents three different schemes based on combinations of ANN, DFT and DWT for fault location in MTDC systems. Despite the contributions and promising results presented by these works, all of them have at least one of the following disadvantages: (a) designed and tested by using only one type of HVDC system (CSC or VSC) (Ye et al., 2021; Yang et al., 2017; Rohani & Koochaki, 2020; Lan et al., 2019; Hao et al., 2018; Ankar & Yadav, 2020; Silva et al., 2019; Arita Torres et al., 2022), (b) based on current signals, which are more susceptible to load conditions and have a wide variation range (Yang et al., 2017; Rohani & Koochaki, 2020; Hao et al., 2018; Ankar & Yadav, 2020; Arita Torres et al., 2022), (c) require communication link to process the signal from the remote terminal (Ye et al., 2021; Lan et al., 2019), (d) use a high sampling frequency, implying a more powerful and complex hardware (Ye et al., 2021; Lan et al., 2019; Hao et al., 2018; Silva et al., 2019).

In this context, a new method based on deep neural networks and DC voltage harmonic content for fault location in HVDC systems is proposed in this paper, aiming to provide a robust solution where pre-fault conditions, fault distance and fault resistance have minimal impact on the method's performance. The method takes advantage of the high capability of neural networks for pattern recognition, associating the harmonic content to a specific fault location. The proposed solution is suited for both VSC and CSC-HVDC systems and is based only on voltage measurements. The main motivation for proposing this solution is to capture a fault location signature contained in the frequency spectrum of faulted voltage signal, assuming that for each fault location there is only one distinct frequency spectrum. Therefore, by using a reasonable sampling frequency the voltage samples acquired at the rectifier substation will be processed by using fast Fourier transform, allowing that a previous trained ANN makes an association between the obtained frequency spectrum and the fault distance on the DC transmission line.

A comparison among the mentioned references and the proposed work is shown in Table 1, highlighting that the proposed method has shown the capability to operate in CSC and VSC-HVDC systems, while there is no evidence that the other methods are able to operate considering both technologies.

It is well known that differently from shallow ANNs, limited to few layers and neurons, deep neural networks (DNNs) have much more complex structures with several layers and neurons by layer. This characteristic makes the DNN capable of handling very large and high-dimensional datasets, being able to deal with complex real-world problems. Therefore, this work proposes a DNN-based method to locate faults in DC transmission lines. The main concept behind this method is to identify fault signatures contained in the frequency spectrum of the DC voltage signal. By using this procedure, the proposed method presents the following advantages: It uses only local DC voltage signals, already available in the rectifier substation; it requires a reasonable sampling frequency; it does not need communication link; it was tested considering VSC and CSC-HVDC system technologies; it presents a robust behavior against different pre-fault conditions and high values of fault resistance. Given the complexity of modern power systems, especially HVDC systems based on converter stations, the development and validation of new solutions play a crucial role in overcoming the barriers raised by the sector's conservatism, which is adapted to conventional methods that often present limitations when applied to modern power grids.

By considering the main advantages of the proposed method, its main contributions are:

- The new method is based on deep neural networks and DC harmonic voltage content, relating fault location to patterns in frequency spectrum;
- The proposed solution is suitable for both VSC and CSC-HVDC systems, consistently demonstrating good performance regardless the fault characteristics or pre-fault conditions;
- Since only DC voltage measurements are used, the transducer specification is less critical than that of current transducers. Indeed, voltage signal exhibits less variation during normal operation and against fault conditions when compared with current signal;

Table 1 Comparison of different fault location methods

Method	Input Signals	Sampling Frequency (kHz)	Link Required	Fault Resistance (Ω)	Error (%)	Used Technique	Tested Technology
[4]	V	20	Yes	10 K	0.1615	DWT and DBN	VSC
[5]	I	10	No	100	1.6	FFT and ANN	VSC
[6]	I	NA	No	10	0.8774	ANFIS	VSC
[7]	V	100	Yes	5.2 k	0.1683	CNN	CSC
[8]	I	1000	No	500	0.46	HHT and SVR	VSC
[11]	V and I	1	No	150	0.041	GPR	CSC
[12]	V	20	No	100	5.69	ANN	CSC
[13]	I	10	No	100	1.7	DWT and ANN	VSC
Proposed	V	10	No	100	$< 2^{(1)}$	ANN	VSC and CSC

NA Not Available; $^{(1)}$ Average error considering VSC and CSC technologies

- The proposed method employs a reasonable sampling frequency (10 kHz) without needing a communication link. By using only local signals and existing hardware resources in the rectifier substation the solution can be considered for practical applications.

This paper is organized as follows: In Sect. 2, the VSC-HVDC system adopted to develop the proposed method is presented and the fault signal characterization is performed. In Sect. 3, the proposed DNN-based method is discussed, including the training process and the preprocessing steps. In Sect. 4, the proposed solution is evaluated, by analyzing the results of thousands of different fault cases. In Sect. 5, the proposed method is validated against a CSC-HVDC system, showing its accuracy and robustness. Finally, the conclusions are drawn in Sect. 6.

2 Fault Signal Characterization

Figure 1 presents the VSC-HVDC system adopted for this study. The electrical system is a symmetric monopole topology with three-level neutral point clamped (NPC) and 12-pulse converters on the rectifier and inverter sides. The substations are connected to AC equivalent systems represented by nominal voltages of 230 kV (50 Hz) and short-circuit powers of 2000 MVA. The nominal voltage in the DC link is ± 100 kV and the rated transmission power is 200 MVA. For modeling the DC transmission line 40 "pi" sections were used, thus representing the distributed nature of its parameters more closely (Merlin et al., 2022; Khatir et al., 2006).

Table 2 Fault cases in the VSC-HVDC system

Case	Type of Fault	Fault Resistance (Ω)	Fault Location
1	PG	0.1	20% of the DC Line
2	PG	10	20% of the DC Line
3	PG	50	20% of the DC Line
4	PG	0.1	50% of the DC Line
5	PG	10	50% of the DC Line
6	PG	50	50% of the DC Line
7	PG	0.1	80% of the DC Line
8	PG	10	80% of the DC Line
9	PG	50	80% of the DC Line

PG Positive pole-to-ground fault

Several fault cases were simulated in the DC line, assuming different fault resistances and fault locations for positive pole-to-ground faults (PG). The simulated scenarios are shown in Table 2. The simulation time is 2.7 s and the fault is always applied at 2.5 s. The analyses are performed by considering the pre- and post-fault periods of 10 ms and 20 ms, respectively.

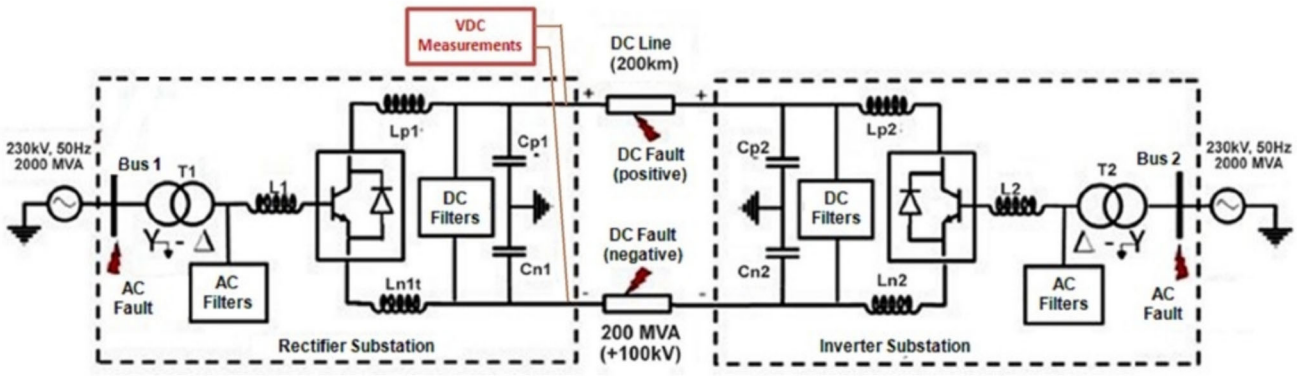

Fig. 1 Adopted VSC-HVDC system

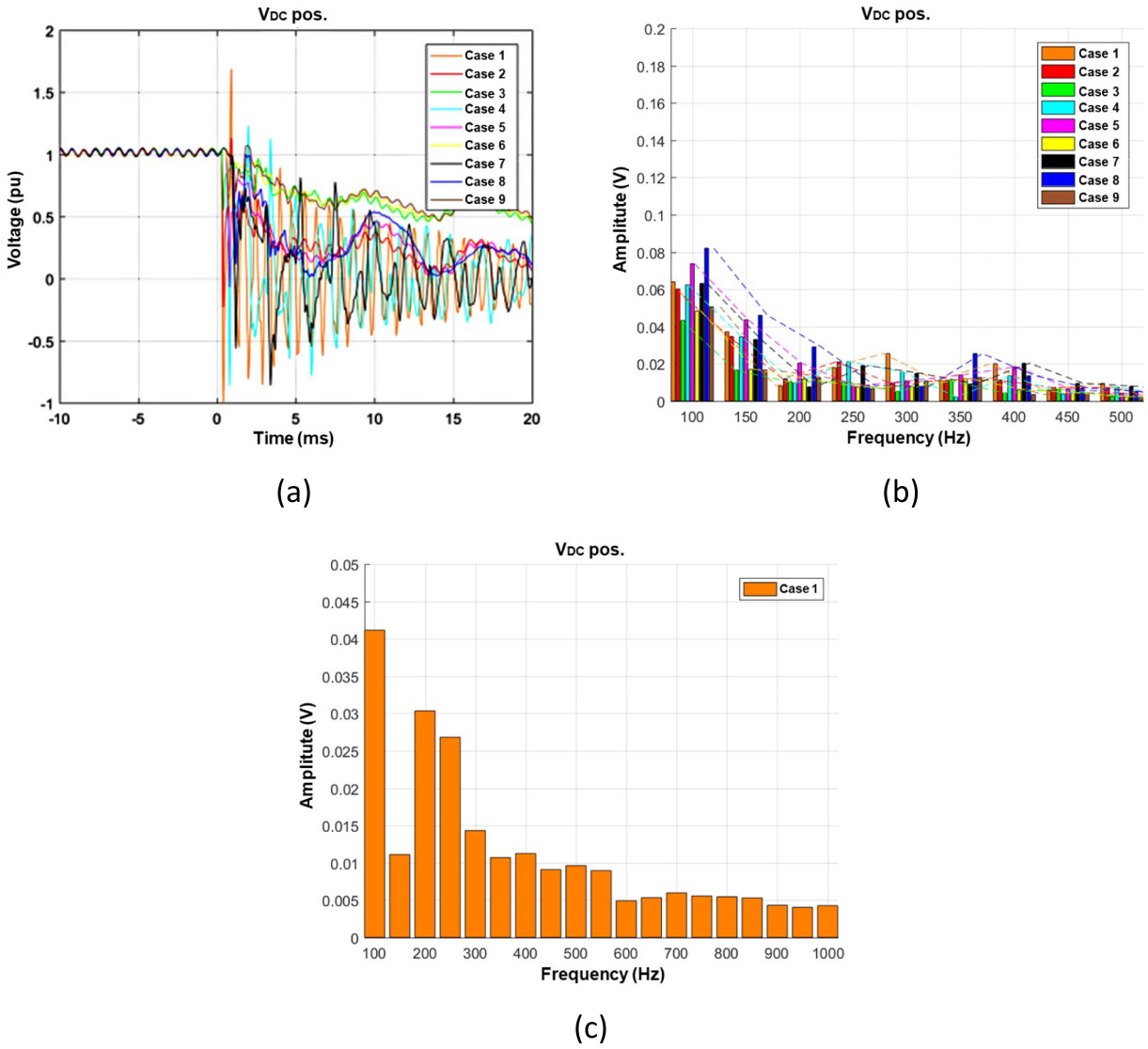

Fig. 2 Fault cases considering: (**a**) DC voltage signals in time domain; (**b**) DC voltage signals in frequency domain; (**c**) limits of relevant frequencies

As it can be seen in Fig. 2a, there is a unique faulted signal for each fault case, which can be associated as a fault signature. However, by analyzing these signals as time functions, the relationship between fault location and faulted signals seems very complex, and almost impossible for dozens or hundreds of cases. In general terms, after a fault event, it is possible to observe a voltage reduction, followed by an oscillatory behavior produced by the discharge of energy stored in the DC line at the fault instant. Such a phenomenon produces traveling waves that travel from the fault point to the DC line terminals in both directions (Anderson et al., 2021; Silva et al., 2019).

On the other hand, by plotting the voltage signals in frequency domain, as shown in Fig. 2b, a more regular pattern can be observed for fault location purposes, i.e., there is only one set of harmonic content related to each simulated fault.

It is important to mention that by means of previous analyzes, based on hundreds of computational simulations using PSCAD, it was verified that the relevant information about the fault event is found until the 10th harmonic, as illustrated in Fig. 2c. The frequency components were extracted by using DFT and the sampling rate of 10 kHz. After this range, the frequency spectrum does not change significantly, which means that there is no relevant information for the purpose of this work.

Some studies found in literature, based on Similarity concept (Farshad & Sadeh, 2013) or ANNs (Silva et al., 2019), have been used for fault location in time domain. Nevertheless, they have important drawbacks with respect to their practical implementation, as they are designed and tested only to address the fault location issue in a particular technology of HVDC system (VSC or CSC). Differently from these methods, the solution presented here is able to work considering VSC and CSC-HVDC systems, without loss of performance. To achieve this goal the proposed method works in frequency domain, taking advantage of the high capability of ANNs for pattern recognition, associating each set of harmonic content to a specific fault location.

Given the complexity of this function, considering both VSC and CSC-HVDC systems, different operating conditions, fault resistances and fault locations, a deep neural network (DNN) is used, thus allowing capturing all relevant information available in the voltage signal. The use of voltage signal results in a more robust solution, when compared to current signal, once the voltage is less susceptible to load condition and varies in a lower range during fault condition.

3 Proposed Method for Fault Location

Figure 3 gives an overview of the proposed method. As can be seen, the DNN is responsible for estimating the fault distance based on a set with eleven frequency components, which works as a kind of fault signature.

In the proposed method, to extract the frequency components, a data window of 20 ms is adopted, assuming 50 Hz as the fundamental frequency. For this purpose, it was used a DFT where a moving data window is updated at each 0.5 ms for the next 10 ms post-fault, thus totalizing 20 frequency spectrums used to feed the trained DNN. Therefore, the DNN is fed with 220 frequency magnitudes from 0 to 10th order.

It is important to mention that this method is exclusively designed for fault location in DC transmission lines, acting only after the fault detection and classification functions, which could be performed by different methods (Arita Torres et al., 2022; Merlin et al., 2022). In fact, this study can be seen as an extension of Merlin et al. (2022), which, operating in the time domain and using shallow ANNs, can trigger the proposed intelligent fault location scheme. For the purpose of this study, a fault is declared when the difference between two consecutives DC voltage samples drops more than 0.01 pu. The DNN is composed of five hidden layers, properly trained to issue a value between 0 and 1, proportional to the transmission line length, e.g., an output of 0.5 represents a fault in the middle of the transmission line, while an output of 1 represents a fault at the remote terminal. Figure 4 exemplifies the operation of the proposed method for fault location.

It is worth noting that there are three different DNNs, but only one of them is enabled after the fault classification function. Each DNN is responsible for a specific fault type (PG—positive pole to ground, NG—negative pole to ground or PN—positive pole to negative pole). In turn, depending on the type of fault, different input signals are used, i.e., PG faults require voltage measurements from positive pole, while NG faults require voltage measurements from negative pole. The designed DNNs for fault location are designated as follows:

- **DNN DIST PN/PNG:** Responsible for estimating the fault distance for faults between the positive and negative poles (with or without the ground involvement);
- **DNN DIST NG:** Responsible for estimating the fault distance for faults between the negative pole and ground;
- **DNN DIST PG:** Responsible for estimating the fault distance for faults between the positive pole and ground.

3.1 DNNs Topologies

As it is well known when working with ANNs, their topologies are defined by a trial-and-error process. Therefore, as a preliminary analysis, a large number of simulations were executed and analyzed, seeking to define the best DNN topology to perform the fault location function in DC transmission

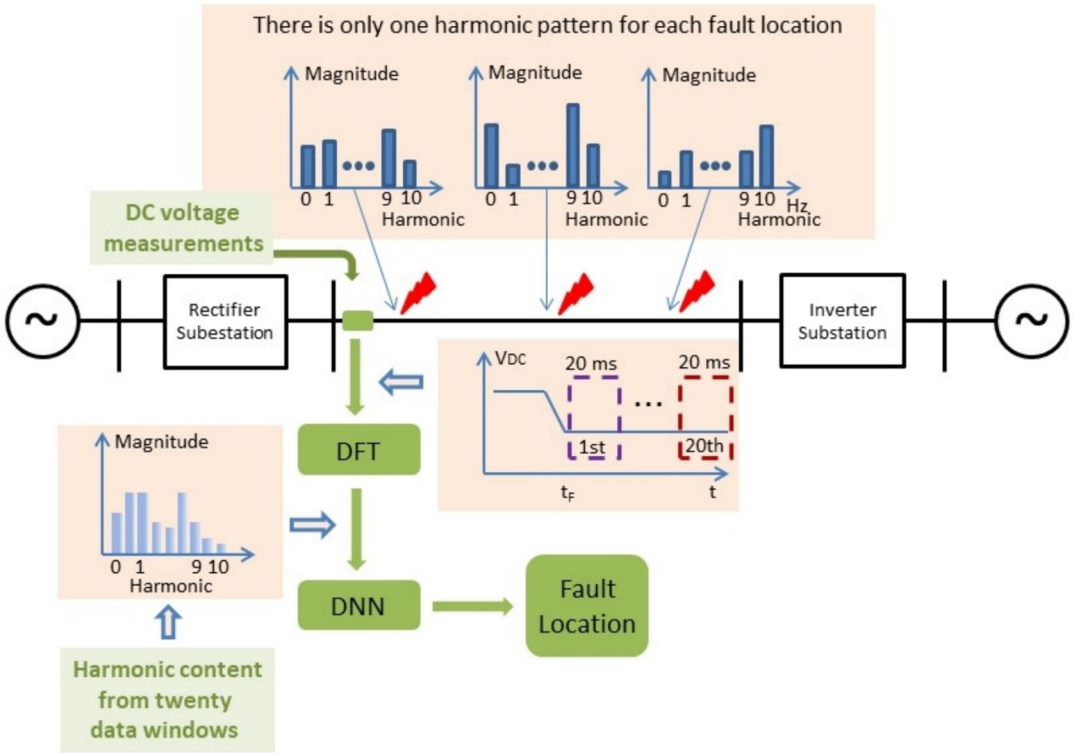

Fig. 3 General view of the proposed method

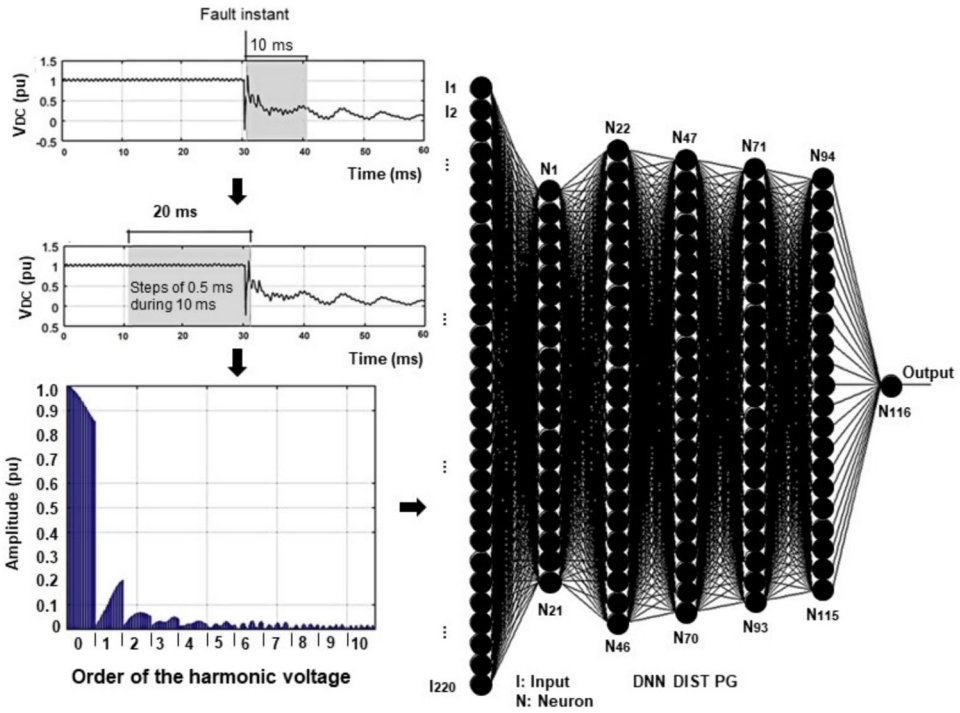

Fig. 4 Operation of the proposed method

Table 3 Topologies of the DNN for fault location

System	DNN	Input	Neurons per Layer					
			First	Second	Third	Fourth	Fifth	Sixth
VSC	DIST PN/PNG	220	19	23	22	21	20	1
	DIST PG	220	21	25	24	23	22	1
	DIST NG	220	20	24	23	22	21	1

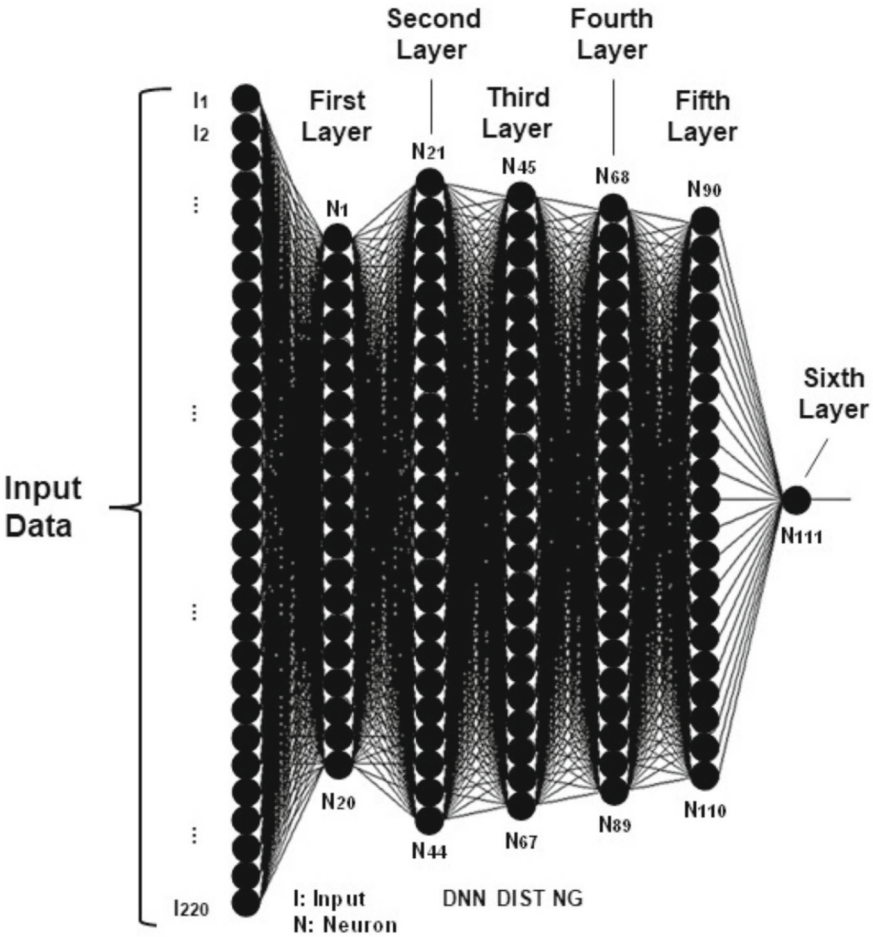

Fig. 5 Topology of the DNN to locate NG faults

lines. The best results were obtained by using six layers (five hidden layers and one output layer), with different number of neurons per layer, according to Table 3.

Despite the different number of neurons per layer, the DNNs are similar with respect to their topology, since assuming n_1 the number of neurons in the first layer, the numbers of neurons (n_2, n_3, n_4 and n_5) in the other layers are as follows: $n_2 = n_1 + 4$; $n_3 = n_1 + 3$; $n_4 = n_1 + 2$; and $n_5 = n_1 + 1$. As an example, Fig. 5 presents the DNN designed to locate NG faults in the adopted VSC-HVDC system (DNN DIST NG). The topology of this DNN is 20–24-23–22-21–1, which is exactly the same as the DNN used to locate NG faults in the adopted CSC-HVDC system, as it will be discussed later.

As an example, the matrices (1) to (3) show the weights and bias for the first, second and sixth layers, respectively. Table 4 summarizes the DNN (in terms of matrices' dimensions) used in this research, highlighting that the neurons from the first layer to the fifth layer are implemented with hyperbolic tangent as activation function, while for the sixth layer was used the linear function. After training the DNN, the weights and bias assume suitable values to perform the fault location, which means that these values represent the stored knowledge. In general, the more elements, the more complex are the regions represented by DNNs.

Table 4 Matrices' dimensions of the DNN for fault location

	1st Layer	2nd Layer	3rd Layer	4th layer	5th Layer	6th Layer
Matrix of Weights	[220 × 20]	[20 × 24]	[24 × 23]	[23 × 22]	[22 × 21]	[21 × 1]
Matrix of Bias	[20 × 1]	[24 × 1]	[23 × 1]	[22 × 1]	[21 × 1]	[1 × 1]

$$\mathbf{W}^1 = \begin{bmatrix} W^1_{1-1} & \cdots & W^1_{1-20} \\ \vdots & \ddots & \vdots \\ W^1_{220-1} & \cdots & W^1_{220-20} \end{bmatrix}_{220x20} \quad \mathbf{B}^1 = \begin{bmatrix} B^1_1 \\ \vdots \\ B^1_{20} \end{bmatrix}_{20x1} \tag{1}$$

$$\mathbf{W}^2 = \begin{bmatrix} W^2_{1-1} & \cdots & W^2_{1-24} \\ \vdots & \ddots & \vdots \\ W^2_{20-1} & \cdots & W^2_{20-24} \end{bmatrix}_{20x24} \quad \mathbf{B}^2 = \begin{bmatrix} B^1_1 \\ \vdots \\ B^1_{24} \end{bmatrix}_{24x1} \tag{2}$$

$$\mathbf{W}^6 = \begin{bmatrix} W^6_{1-1} \\ \vdots \\ W^6_{21-1} \end{bmatrix}_{21x1} \quad \mathbf{B}^6 = \begin{bmatrix} B^1_1 \end{bmatrix}_{1x1} \tag{3}$$

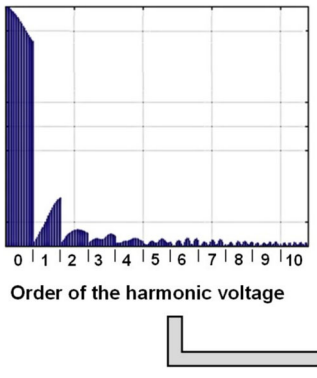

Order	Samples	Frequency (
0	0 to 20	0
1	21 to 40	50
2	41 to 60	100
3	61 to 80	150
4	81 to 100	200
5	101 to 120	250
6	121 to 140	300
7	141 to 160	350
8	161 to 180	400
9	181 to 200	450
10	201 to 220	500

Fig. 6 Harmonic content to feed the DNNs

3.2 Input Signals to Feed the Specified DNNs

The adopted data window is built by DC voltage samples, acquired during 10 ms post-fault and sampled at 10 kHz. Many different methods could be used for fault detection, but for the purpose of this work, a DC voltage drop higher than 0.1 pu was employed to declare a fault condition. It is important to note that the main goal of this work is to propose an accurate and reliable fault location method, regardless of the previous steps of fault detection and classification, which are exhaustively discussed in literature. After each 10 ms, the DFT is applied on the data window (which is updated at each 0.5 ms), generating 20 frequency spectrums from 0 to 10th order. Thus, these 220 frequency components (11 frequency components × 20 windows) are used to feed the DNN, as illustrated in Fig. 6.

3.3 Definition of the Training Sets for Fault Location

As discussed in the previous sections, only DC voltage signals already available in the rectifier substation are used by the proposed method. These signals are designated as follows:

- Vpos—positive pole-to-ground voltage
- Vneg—negative pole-to-ground voltage

The training sets are built considering twenty data windows with the harmonic content (from 0 to 500 Hz) present in Vpos or Vneg, depending on the fault type. The following situations were considered to generate the fault cases for training purposes, highlighting that 1000 simulations were performed for each fault type, as follows:

Table 5 Parameters for building the training sets and test cases

Parameter	Minimum Value	Maximum Value
Voltage at the bus 1 (pu)	0.95	1.05
Voltage at the bus 2 (pu)	0.95	1.05
Power across the line (pu)	0.5	1
Fault location in the DC line (pu)	0	1
Fault resistance (Ω)	0	100
Voltage angle at the bus 1 (°)	0	360
Voltage angle at the bus 2 (°)	0	360

- Positive pole to negative pole fault
- Positive pole to negative pole-to-ground fault
- Positive pole-to-ground fault
- Negative pole-to-ground fault

In addition to the fault type, the variables and ranges shown in Table 5 were used for generating the training sets. It is important to mention that the same ranges were used for generating the test cases, but considering different values, as will be discussed in the next section. Thus, the proposed method will be always tested by means of unknown operating scenarios.

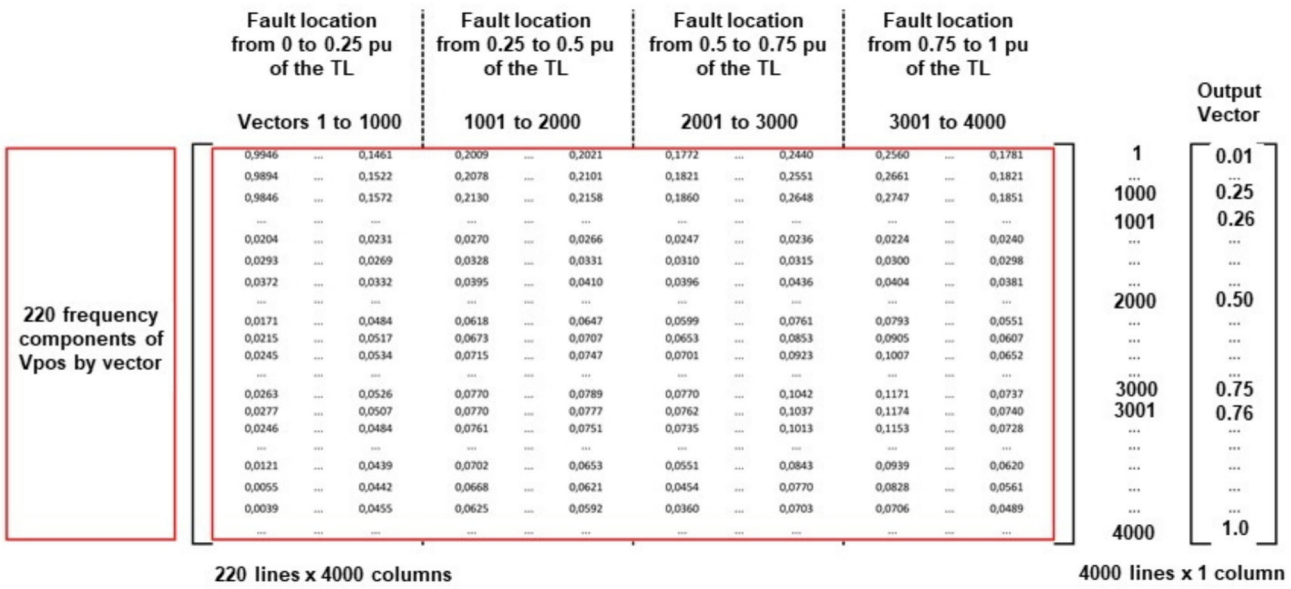

Fig. 7 Training set for the DNN DIST TL PN/PNG

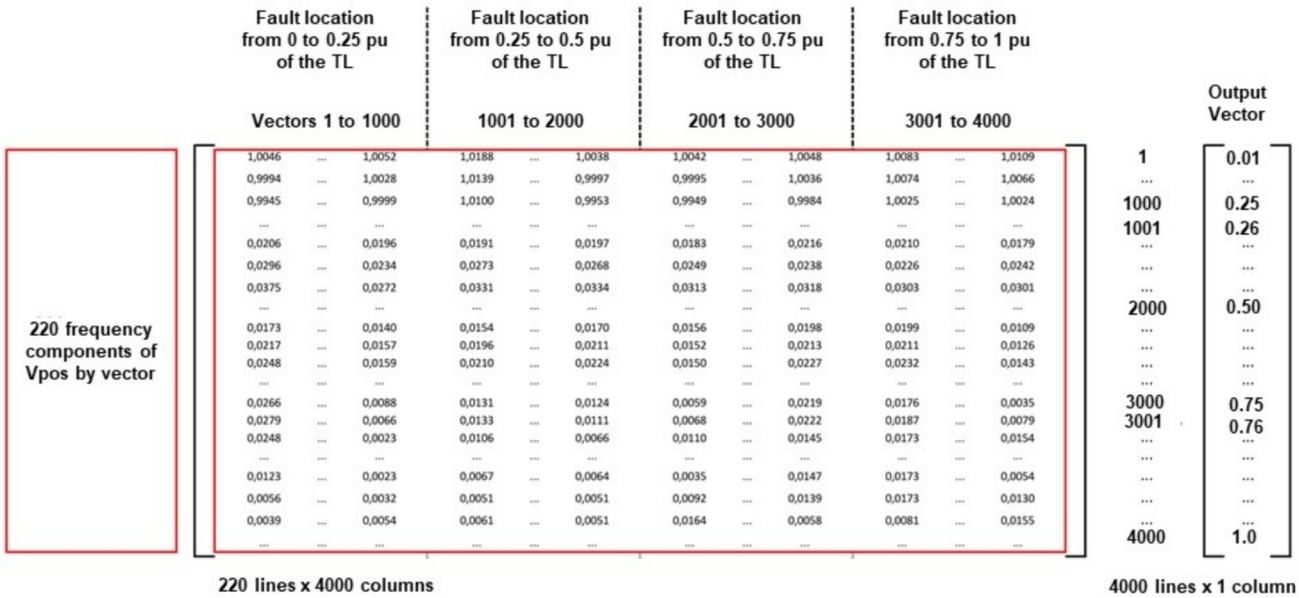

Fig. 8 Training set for the DNN DIST TL PG

Once the training sets were built, the three DNNs to locate PN/PNG, PG and NG were trained. They work totally independent of each other, which means that each one is responsible for a specific fault type, as follows:

- **DNN DIST PN/PNG:** DNN responsible for fault location when the fault involves the positive and negative poles (with and without ground involvement), responding with a value between 0 and 1, depending on the fault distance with respect to the rectifier substation. Thus, for faults at the beginning of the DC transmission line, the DNN issues 0, while for faults at the end of the DC transmission line the DNN issues 1.
- **DNN DIST PG:** DNN responsible for fault location when a positive pole-to-ground fault takes place in the DC transmission line, responding with a value between 0 and 1, depending on the fault distance with respect to the rectifier substation.
- **DNN DIST NG:** DNN responsible for fault location when a negative pole-to-ground fault takes place in the DC transmission line, responding with a value between 0 and 1,

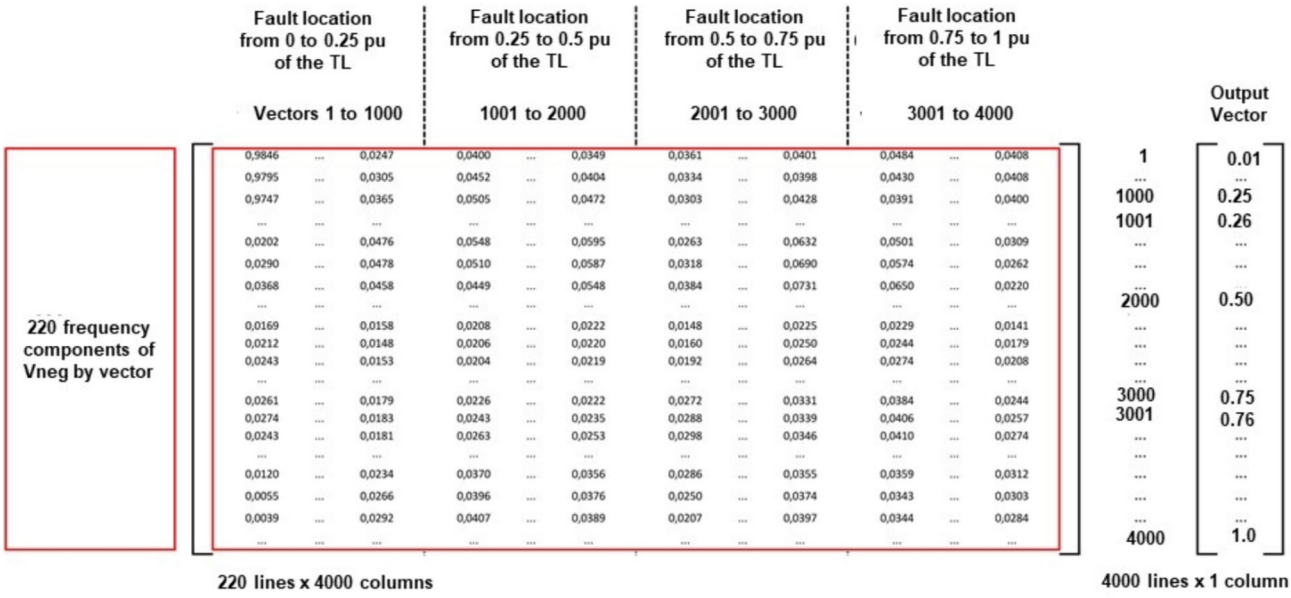

Fig. 9 Training set for the ANN DIST TL NG

Table 6 Performance of the proposed method

	Fault types in the DC transmission line			
	PN	PNG	PG	NG
Number of Cases	500	500	1000	1000
Hit Rate	493 (98.6%)	494 (98.8%)	992 (99.2%)	987 (98.7%)
Fail Rate	7 (1.4%)	6 (1.2%)	8 (0.8%)	13 (1.3%)

depending on the fault distance with respect to the rectifier substation.

Figures 7, 8 and 9 are suitable to better illustrate the DNNs' training sets. In a simplified way, these figures show the training sets for the DNN DIST PN/PNG, DNN DIST PG and DNN DIST PN, respectively.

After a large number of simulations and analyses, the best trade-off between performance and computational burden was verified for the DNNs topologies shown in Table 3, considering the possible fault types. This means that DNNs more complex than the selected ones work and could be adopted, but they would require more processing power without significantly improving the performance. On the other hand, DNNs smaller than the selected ones have their performance degraded, despite requiring less processing power.

4 Fault Location in the DC Transmission Line

For evaluation purposes, by considering the ranges presented in Table 5, the proposed method was tested against 3000 different fault cases in the DC line, distributed as follows:

- PN (positive to negative ground fault): 500 cases
- PNG (positive to negative to ground fault): 500 cases
- PG (positive to ground fault): 1000 cases
- NG (negative to ground fault): 1000 cases

In addition to the fault type, the fault cases were generated assuming the variables and ranges shown in Table 1. The proposed method is evaluated with respect to its accuracy for fault location. The relative error in estimating the fault distance is given by (4), where D_{act}, D_{est} and L correspond to the actual fault distance, the estimated fault distance and the total TL length, respectively.

$$E(\%) = \frac{D_{act} - D_{est}}{L} \cdot 100 \tag{4}$$

As an additional measure of the method's performance, a threshold value of 5% is adopted, i.e., for errors higher than this threshold the distance estimation is considered wrong and a failure is registered, while for errors lower than 5% the distance estimation is considered successful (Santos & Senger, 2011; Brahma & Girgis, 2004; Petite et al., 2021; Akdağ et al., 2024). Table 6 shows the overall performance of the

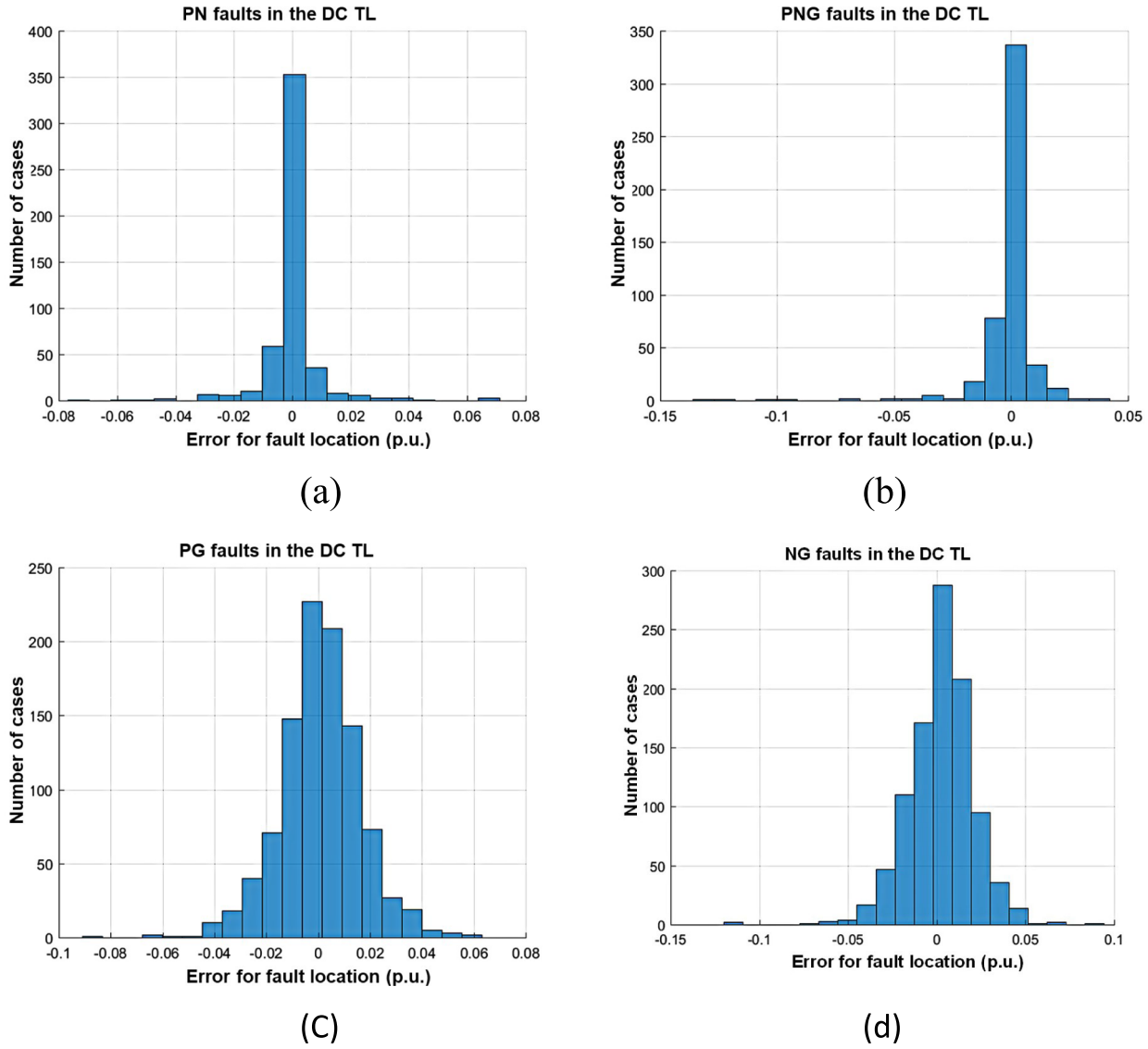

Fig.10 Errors distribution for: **a** PN faults; **b** PNG faults; **c** PG faults; and **d** NG faults

proposed method for 3000 fault cases in the DC transmission line, with emphasis on pole-to-ground faults, as they are much more frequent than pole-to-pole faults in HVDC systems and are the main concern of protection engineers. The errors distribution for each fault type is presented in Fig. 10.

By analyzing Fig. 10, it is possible to observe the high level of accuracy is achieved with the solution presented here. In general terms, faults involving both poles are similar with most errors, around ± 2%, while pole-to-ground faults are similar with most errors between ± 5%. Moreover, it is worth noting that the few observed fault location errors are lower than 8% for PG faults, 15% for PGN faults, 9% for PG faults and 12% for NG faults.

5 A Factors Affecting the Method's Performance

This subsection analyzes how the proposed method is affected by factors as fault resistance and fault distance. For this purpose, as an example, Fig. 11a illustrates the relationship between fault resistance and fault location for PG faults, showing that the vast majority of the tested cases present errors lower than 5%, regardless of the fault resistance value. Nonetheless, for more information about this relationship, the 3D figure might not be suitable, being replaced by its 2D version, as shown in Fig. 11b. This figure allows a more detailed visualization, where one can see that for PG faults, assuming fault resistance of 80 Ω, 80% and 100% of the tested cases present errors lower than 2% (point A) and 4%

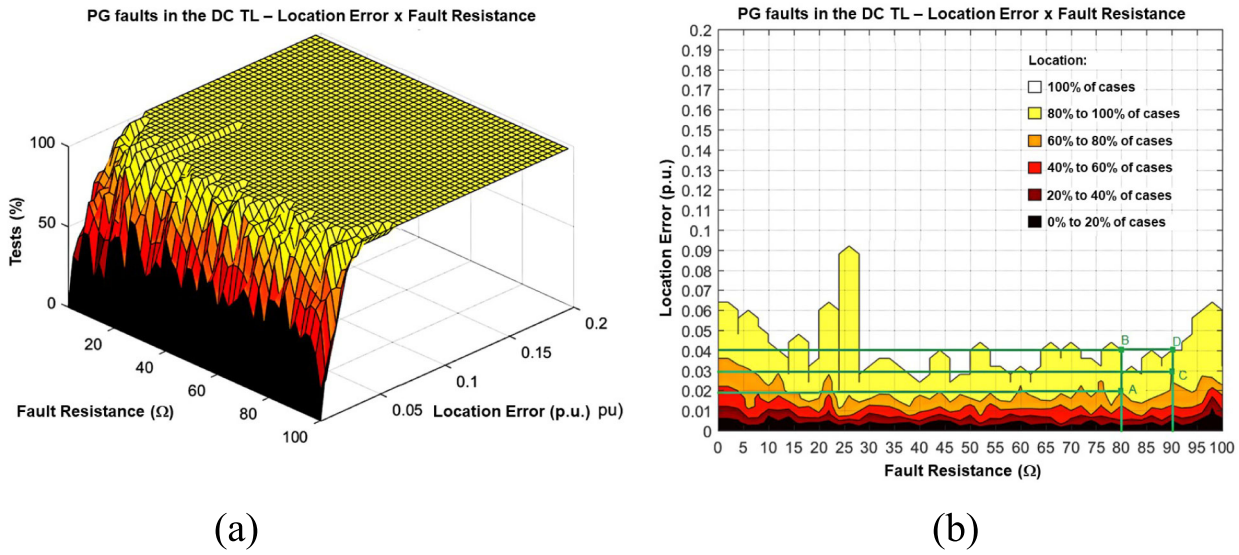

(a) (b)

Fig. 11 Relationship between fault resistance and fault location in: **a** 3D view and **b** 2D view

(point B), respectively. On the other hand, assuming the same type of fault, but with a fault resistance of 90 Ω, it is possible to verify that 80% and 100% of the tested cases present errors lower than 3% (point C) and 4% (point D), respectively.

Figure 12 presents the effect of the fault resistance on the method's performance for PN, PNG, PG and NG faults, in a total of 3000 fault cases, i.e., 500 cases for PN and PNG faults and 1000 cases for PG and NG faults, respectively. As can be seen in Fig. 12, there is not any significant dependence between fault resistance and fault location for DC line faults.

On the other hand, when analyzing the method performance with respect to the fault distance, it is possible to verify a dependency between them, as the errors are higher for faults close to the DC line terminals, as shown in Fig. 13. However, it is important to note that the error is still lower than 5% for more than 90% of the fault cases.

6 Validation of the Proposed Method

A new HVDC system, based on CSC technology, is modeled and simulated to validate the proposed method. Thus, this new system allows generating 5000 different fault cases to measure the robustness and comprehensiveness of the solution presented here. Once again, the fault cases were generated assuming the variables and ranges shown in Table 4.

The new CSC-HVDC system is shown in Fig. 14. This system is connected to an AC equivalent source of 500 kV at 60 Hz and short-circuit level of 5000 MVA on the rectifier side and connected to an AC equivalent source of 345 kV at 50 Hz and short-circuit level of 10,000 MVA on the inverter side. The nominal voltage of the DC link is ± 500 kV, and the rated transmission power is 1000 MVA. The DC transmission line of 300 km length was modeled in Power System Toolbox (MATLAB) by using 40 "pi" sections, thus allowing representing the distributed nature of its parameters more closely (Merlin et al., 2022; Khatir et al., 2006). As assumed before, fault cases are characterized by short-circuits between positive pole and ground along the DC line, as depicted in Fig. 14. Once again, the relative error in estimating the fault distance is calculated by (1).

As it can be seen in Fig. 14, only positive pole-to-ground faults are considered for the adopted CSC-HVDC system. The procedure for training the DNN and for defining its topology is exactly the same already discussed in the sub-Sect. 3C, when considering PG faults and DNN DIST PG. These characteristics simplify the practical implementation of the proposed method, enabling its use in different scenarios.

For the CSC-HVDC system, the observed results were better than the ones observed for the VSC-HVDC system, as all faults were accurately located. With respect to the adopted criterion, this means that all faults were located with an error lower than 5%. Figure 15 shows that the errors are mostly concentrated between ± 1%.

More details about the method performance can be seen in Fig. 16 and Fig. 17. By analyzing Fig. 16, it is possible to verify that the errors are higher for fault resistances smaller than 2Ω. With respect to fault location, Fig. 17 shows that the errors are higher for fault cases close to the rectifier substation (up to 3% of the DC line). However, it is worth noting that in both analyses, the errors are still lower than 5%. For all other fault cases, the errors are lower than 2%.

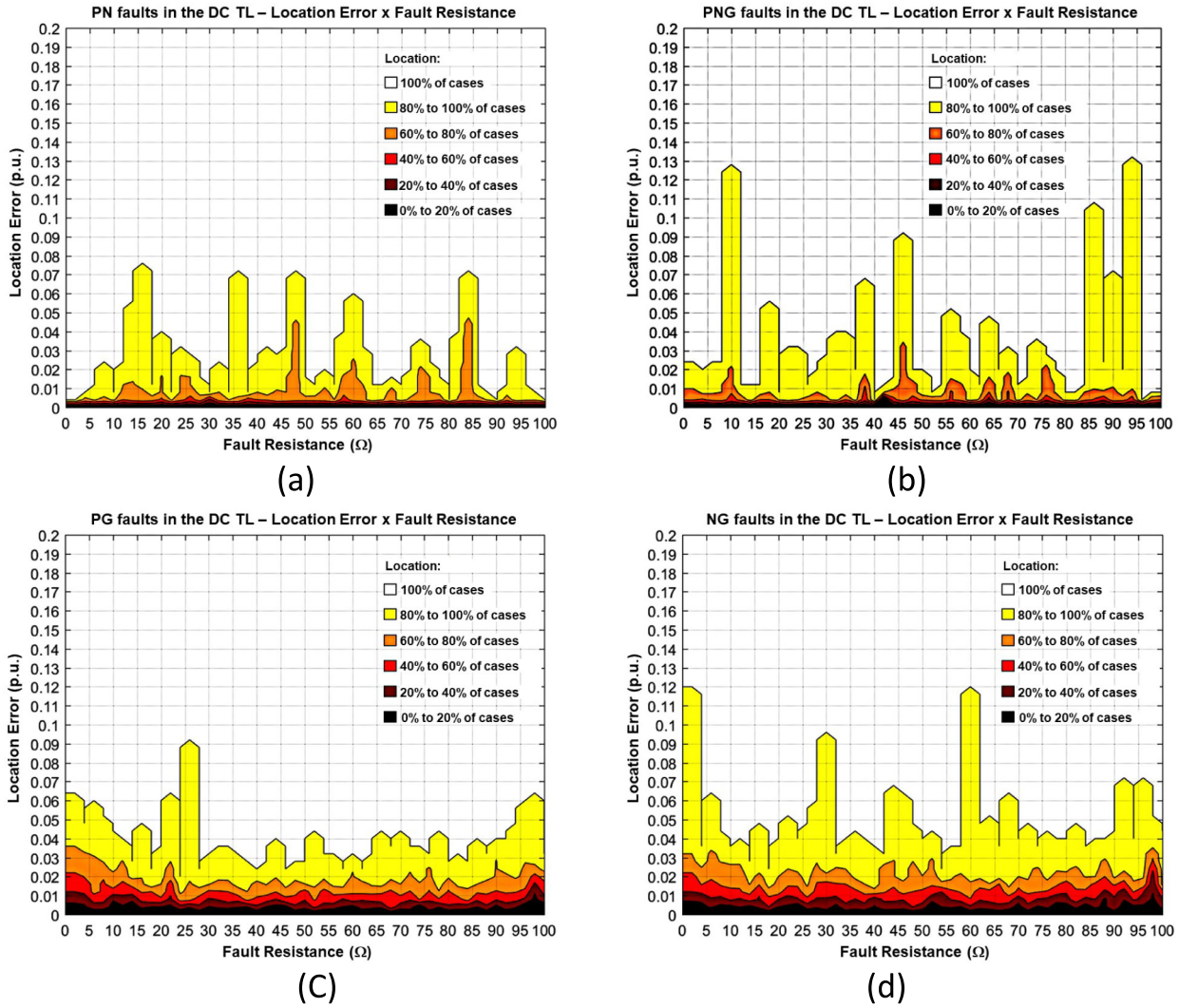

Fig. 12 Fault resistance effect on proposed method considering: (**a**) PN faults; (**b**) PNG faults; (**c**) PG faults; and (**d**) NG faults

It is important to mention that for VSC and CSC-HVDC systems similar to the adopted ones, the proposed method can be applied without loss of performance. Nevertheless, for HVDC systems with significant differences from the adopted ones, i.e., with different topologies (multi-terminal, existence of current limiters or other filters) a new training process must be performed, thus defining a new workspace. Similarly, a new training process is required to improve the method's performance for fault resistances higher than 100 Ω, which was defined as the upper limit in this study. These could be considered as the limitations of the current version of the proposed method.

After analyzing the obtained results for both VHDC systems, it was observed that this intelligent location method is able to work properly only by using voltage signals captured with a reasonable sampling frequency regardless of the technology (VSC or CSC). Moreover, a high accuracy was always verified against a large number of fault cases considering different fault characteristics. It is important to point out that using only voltage signals the method is less affected by pre-fault or load condition, and the PT specification is not as critical as CT specification.

In a few works, the main novelties of the proposed method are as follows:

- The method based on DNN is able to find signatures in the voltage frequency spectrum;
- The proposed solution is suitable for both VSC and CSC-HVDC systems;
- Only DC voltage is used, and the method is less affected by fault and pre-fault condition;
- A reasonable sampling frequency (10 kHz) is used without needing a communication link.

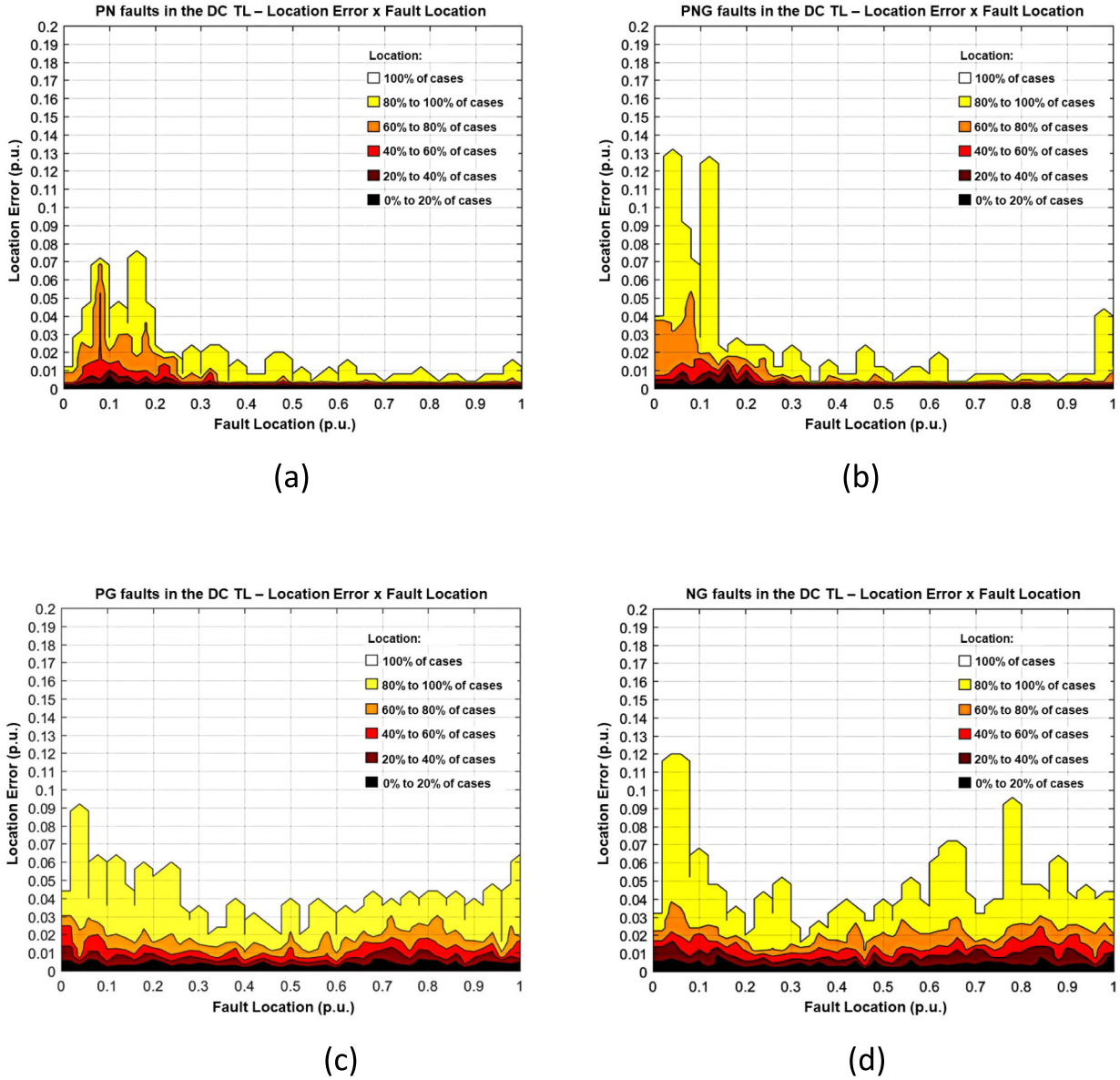

Fig. 13 Fault location effect on proposed method considering: (**a**) PN faults; (**b**)PNG faults; (**c**) PG faults; and (**d**) NG faults

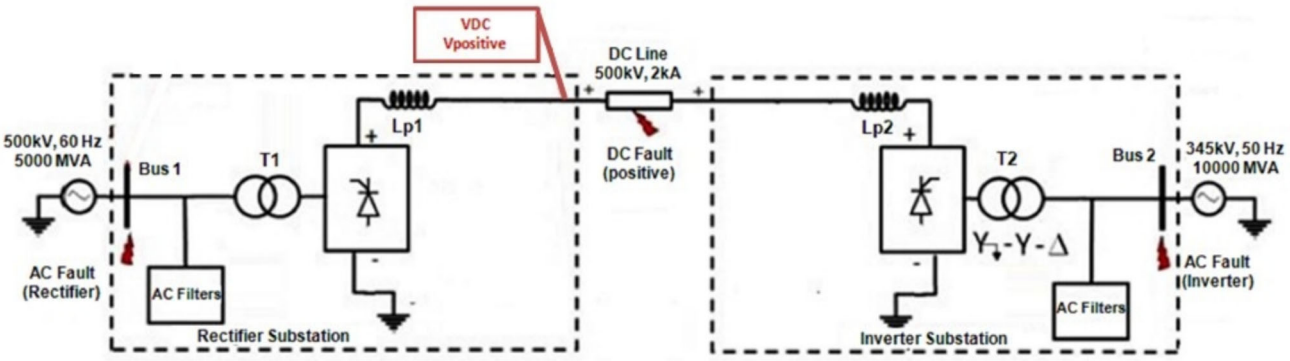

Fig. 14 Adopted CSC-HVDC system to validate the proposed algorithm

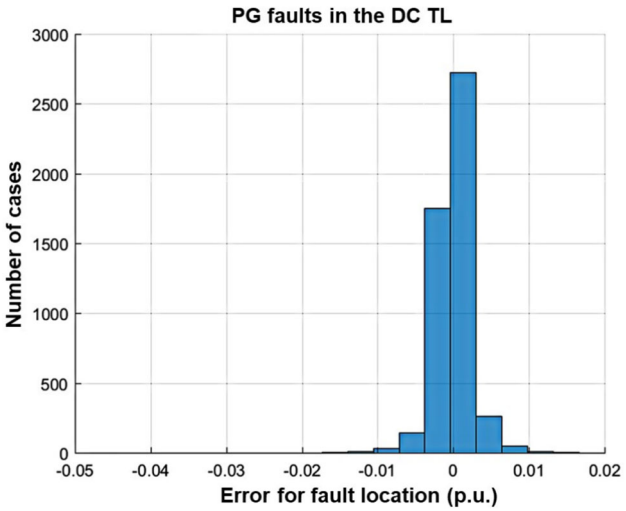

Fig. 15 Error distribution considering the CSC-HVDC system and PG faults

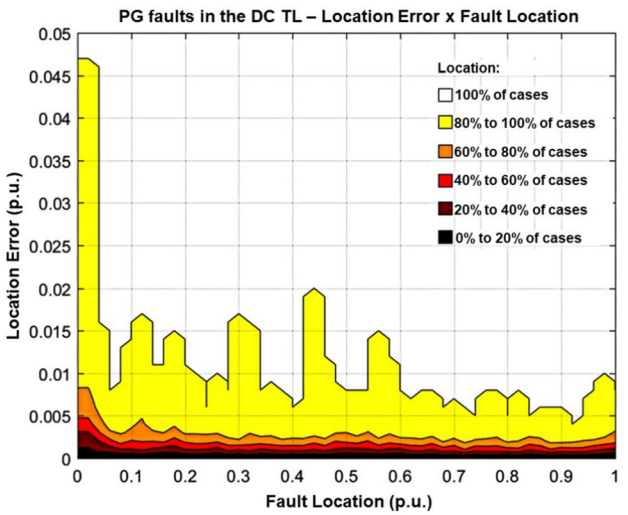

Fig. 17 Fault location effect considering the CSC-HVDC system and PG faults

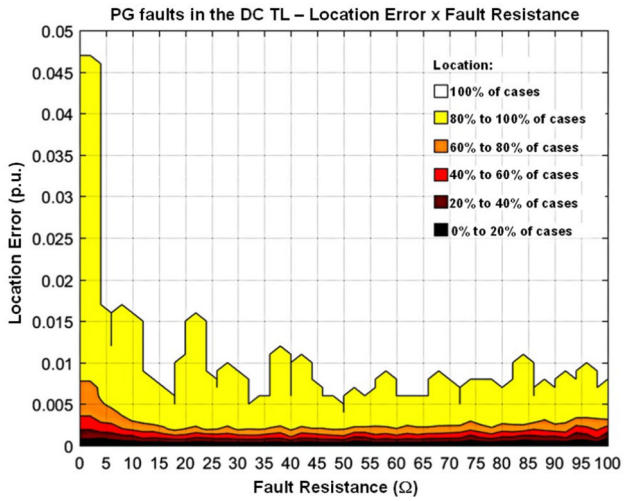

Fig. 16 Fault resistance effect considering the CSC-HVDC system and PG faults

7 Conclusions

This work presented a new fault location method based on DNN for HVDC systems. The proposed method showed an accurate and robust behavior for locating faults in DC transmission lines, regardless of the HVDC technology (VSC and CSC). Despite its accuracy and robustness, the solution presented here has the advantage of using only local DC voltage signals. To extract the harmonic content of the voltage signals, the DFT was applied to a moving data window of 20 ms, by using a sampling frequency of 10 kHz.

The proposed method was evaluated against thousands of test cases, and two different HVDC systems, always presenting an accurate performance. Against 3000 different fault cases from the VSC-HVDC, the error was within 5% in 2966 fault scenarios (Table 6), while against 5000 fault cases from the CSC-HVDC system the error was within 5% in all scenarios, being most of them within 1% (Fig. 15). It is important to mention that both adopted HVDC systems are widely used for developing and testing protection and control algorithms. Given the complexity of the fault location issue in DC transmission lines, as for example, the effect of pre-fault conditions, high values of fault resistance and converter actions, the DNN appears as a very promising solution. This kind of ANN is more complex than the usual shallow ones, so that they are able to capture relevant information by means of a complex architecture composed of a large number of layers and neurons.

It is important to point out that the training procedure and DNN topology specified to be used in the VSC-HVDC system were also used to locate faults in the CSC-HVDC system. This characteristic simplifies the implementation of the proposed solution, which will be the next planned step for this research, i.e., hardware implementation and practical tests by using HIL (hardware-in-the-loop) simulation.

Fault location in HVDC systems still have issues to be addressed, since the converter stations and the adopted HVDC technology can change the dynamic response of the power grid under fault. As future research in this area, new artificial intelligence techniques and hybrid algorithms could be tested, in order to improve the accuracy of fault location methods. Moreover, real fault signals could be used in practical tests, allowing the measure the real benefits of each proposed methods. Another important step of this research would be to verify how the noisy voltage signals affect the proposed method and what its real robustness level against noise.

Authors' Contributions V. M. was involved in conceptualization, methodology, formal analysis, investigation and writing—original draft preparation. R. C. took part in supervision, methodology, analysis, review and editing and project administration. A. P. participated in methodology, analysis, review and editing. J. C. performed methodology, analysis, review and editing.

Funding This project was developed with financial support from the Brazilian government via CAPES (Coordination for the Improvement of Higher Level Personnel), the Ministry of Education of Brazil.

Availability of Data and Materials No datasets were generated or analyzed during the current study.

Declarations

Ethical Approval Not applicable.

Competing Interests The authors declare no competing interests.

References

Abdali, A., Mazlumi, K., & Noroozian, R. (2019). High-speed fault detection and location in DC microgrids systems using multi-criterion system and neural network. *Applied Soft Computing Journal, 79*, 051. https://doi.org/10.1016/j.asoc.2019.03.051

Akdağ, M., Mamiş, M. S., & Akmaz, D. (2024). Enhancing fault location accuracy in transmission lines using transient frequency spectrum analysis: An investigation into key factors and improvement strategies. *Electricity, 5*(4), 861–876. https://doi.org/10.3390/electricity5040043

Anderson, P. M., Henville, C., Rifaat, R., Johnson, B., & Meliopoulos, S. (2021). Power system protection. *Second Edition. In Power System Protection, 14*(11), 4690. https://doi.org/10.1002/9781119513100

Ankar, S. J., & Yadav, A. (2020). A novel approach to estimate fault location in current source converter–based HVDC transmission line by Gaussian process regression. *International Transactions on Electrical Energy Systems, 30*(2), 12221. https://doi.org/10.1002/2050-7038.12221

Arita Torres, J., Santos, R. C., Yang, Q., & Li, J. (2022). Analyses of different approaches for detecting, classifying and locating faults in a three-terminal VSC-HVDC system. *International Journal of Electrical Power and Energy Systems, 135*, 107514. https://doi.org/10.1016/j.ijepes.2021.107514

Brahma, S. M., & Girgis, A. A. (2004). Fault location on a transmission line using synchronized voltage measurements. *IEEE Transactions on Power Delivery, 19*(4), 1619–1622. https://doi.org/10.1109/TPWRD.2003.822532

Farshad, M., & Sadeh, J. (2013). A novel fault-location method for HVDC transmission lines based on similarity measure of voltage signals. *IEEE Transactions on Power Delivery, 28*(4), 2483. https://doi.org/10.1109/TPWRD.2013.2272436

Hao, Y., Wang, Q., Li, Y., & Song, W. (2018). An intelligent algorithm for fault location on VSC-HVDC system. *International Journal of Electrical Power and Energy Systems, 94*, 30. https://doi.org/10.1016/j.ijepes.2017.06.030

Jovcic, D., Baulcombe, P. D., Smil, V., Thomas, L., Hauff, J., Bode, A., Neumann, D., Haslauer, F., Houghton, J., John, T. H. E., Initiative, R. A. Y., Smil, V., Akagi, H., Hirokazu, E., Aredes, M., Small, P., Schewe, P. F., Brennan, T. J., Yergin, B. D., & Bfg, T. (2011). High voltage direct current transmission : converters, systems, and DC grids. *CEUR Workshop Proceedings, 1542*(3), 1024.

Khatir, M., Zidi, S. A., Fellah, M. K., Hadjeri, S., & Dahou, O. (2006). HVDC transmission line models for steady-state and transients analysis in SIMULINK environment. *IECON Proceedings (Industrial Electronics Conference)*. https://doi.org/10.1109/IECON.2006.347234

Lan, S., Chen, M. J., & Chen, D. Y. (2019). A novel HVDC double-terminal non-synchronous fault location method based on convolutional neural network. *IEEE Transactions on Power Delivery, 34*(3), 848. https://doi.org/10.1109/TPWRD.2019.2901594

Li, B., & He, J. (2020). Protection principle and technology of the VSC-based DC Grid. *Springer Singapore*. https://doi.org/10.1007/978-981-15-6644-8

Merlin, V. L., Santos, R. C., Pavani, A. P. G., & Vieira, J. C. M. (2022). A frequency spectrum-based method for detecting and classifying faults in HVDC systems. *Electric Power Systems Research, 207*, 107828. https://doi.org/10.1016/j.epsr.2022.107828

Petite, F. S. V., Santos, R. C., Junior, G. M., Yang, Q., & Li, J. (2021). A comprehensive backup protection for transmission lines based on an intelligent wide-area monitoring system. *International Transactions on Electrical Energy Systems, 31*(5), 12870. https://doi.org/10.1002/2050-7038.12870

Rohani, R., & Koochaki, A. (2020). A hybrid method based on optimized neuro-fuzzy system and effective features for fault location in VSC-HVDC systems. *IEEE Access, 8*, 2986919. https://doi.org/10.1109/ACCESS.2020.2986919

Santos, R. C., & Senger, E. C. (2011). Transmission lines distance protection using artificial neural networks. *International Journal of Electrical Power & Energy Systems, 33*(3), 721–730. https://doi.org/10.1016/j.ijepes.2010.12.029

Silva, A. S., Santos, R. C., Torres, J. A., & Coury, D. V. (2019). An accurate method for fault location in HVDC systems based on pattern recognition of DC voltage signals. *Electric Power Systems Research*, *170*. https://doi.org/10.1016/j.epsr.2019.01.013

Yang, Q., Le Blond, S., Aggarwal, R., Wang, Y., & Li, J. (2017). New ANN method for multi-terminal HVDC protection relaying. *Electric Power Systems Research, 148*, 024. https://doi.org/10.1016/j.epsr.2017.03.024

Yang, Q., Li, J., Le Blond, S., & Wang, C. (2016). Artificial Neural Network Based Fault Detection and Fault Location in the DC Microgrid. *Energy Procedia, 103*, 261. https://doi.org/10.1016/j.egypro.2016.11.261

Ye, X., Lan, S., Xiao, S. J., & Yuan, Y. (2021). Single pole-to-ground fault location method for MMC-HVDC system using wavelet decomposition and DBN. *IEEJ Transactions on Electrical and Electronic Engineering, 16*(2), 238. https://doi.org/10.1002/tee.23290